



# Evolution of Local Strains Under Uniaxial Compression in an Anisotropic Gypsum Sample

Chiara Caselle<sup>1</sup>(✉), Gessica Umili<sup>1</sup>, Sabrina Bonetto<sup>1</sup>,  
Daniele Costanzo<sup>2</sup>, and Anna Maria Ferrero<sup>1</sup>

<sup>1</sup> Department of Earth Science, Università degli Studi di Torino,  
Via Valperga Caluso 35, 10125 Turin, Italy  
chiara.caselle@unito.it

<sup>2</sup> Department of Structural, Geotechnical and Building Engineering,  
Politecnico di Torino, Corso Duca degli Abruzzi 24, 10129 Turin, Italy

**Abstract.** In the fields of geomechanical researches and applications, the study of mechanical properties of rock materials through laboratory tests is a fundamental milestone in the process of understanding and modeling the mechanical behavior and the stability assessment. In particular, the study and quantification, in laboratory samples, of the local strains and of their concentration and localization during the application of an external load may allow for a more accurate description of the material behavior.

In this study, we focused on a specific gypsum rock with a strongly anisotropic structure. The strategic importance of gypsum in the construction industry and its consequent extensive exploitation by both open pit and underground quarries requires a good knowledge of its strength and stress-strain relation. We propose an application of Digital Image Correlation (DIC analysis) to the study of the evolution of local strains in gypsum rock under the application of a uniaxial compression. Resulting maps of local strains were analyzed and interpreted considering the influence of textural variability of the material. In consideration of the material anisotropy, DIC analysis was applied on two adjacent faces of a prismatic sample, allowing for a three-dimensional interpretation of strain evolution.

**Keywords:** DIC analysis · Gypsum rock · Local strains

## 1 Introduction

Measuring and quantifying local strains, their concentration and localization during laboratory tests are important and challenging research topics in rock mechanics. Several techniques have been adopted for this purpose (e.g. optical and electronic microscopy, radiographic analysis, ultrasonic and acoustic techniques, multiple stress and strain local measurements, digital image correlation, x- ray tomography). In particular, Digital Image Correlation (DIC), providing strain values on a grid of the entire surface of the sample for the entire duration of the test, is an innovative technique with large applications in mechanical engineering. DIC is a robust non-contact technique

based on the comparison of subsequent photographic images and the correlation of analogous pixels in consecutive images (Peters and Ranson 1982; Chu et al. 1985; Vend Roux and Knauss 1998; Blaber et al. 2015).

In rock mechanics research field, many attempts to apply DIC technique during loading tests were made, e.g. Ferrero and Migliazza (2009) on marl subjected to uniaxial compression tests, Nguyen et al. (2011) on tuff subjected to plane-strain compression tests, Zhang et al. (2012) on sandstone under indentation, Stirling et al. (2013) on sandstone subjected to Brazilian tests, Yang et al. (2015) on granite subjected to uniaxial traction tests, Vitone et al. (2013) on fissured clays under plane-strain compression.

In the present research, this technique was applied to the quantification and measurement of local strains in gypsum rock. This material has a strategic importance in the construction industry and is, consequently, extensively exploited by both open pit and underground quarries. It is required, therefore, a good knowledge of its strength and strain features.

The open-source, freely available 2D subset-based DIC software package called Ncorr (Blaber et al. 2015) was chosen to process images of a uniaxial test on a prismatic sample of gypsum rock; the evolution of axial and horizontal strains during the test was visualized and described on two adjacent faces of the sample. Results were compared with the textural features of the material.

## 2 Materials and Methods

The studied material is a gypsum rock from Monferrato Area (NW Italy). It can be classified as “branching selenite gypsum” (Lugli et al. 2010).

It is constituted by nodules of clear, elongated gypsum crystals with a mean grain size of 0.5–1 mm, strictly in contact with each other. They are surrounded by anisotomosed layers with finer grain sizes, usually constituted by crystals of gypsum, carbonate and some terrigenous minerals (quartz, feldspars and clays). The structure is therefore strongly anisotropic: a planar anisotropy is identified by the nodules and the surrounding layers and a linear preferential orientation is created by the elongation of gypsum crystals (Fig. 1). This anisotropy, here described at the sample scale, is also evident at the rock-mass scale, where lenticular bodies of selenite gypsum are surrounded by layers of finer material with various thicknesses.

The rock has a mean porosity of 5–6%, a mean solid density of 23–24 kN/m<sup>3</sup> and a mean bulk density of 22 kN/m<sup>3</sup>.

A prismatic sample with sizes of 107 × 50.5 × 55.6 mm was prepared. The upper and lower faces were polished to obtain smooth and parallel planes. The prismatic shape, with four free flat faces of similar sizes, was preferred to the cylindrical one to facilitate the acquisition, during the test, of the photographic images without perspective effects. The choice to have four axial faces with similar sizes instead to enhance one dimension, as in the usual procedure of DIC analysis, was aimed to study two different sides of the sample, in order to describe the strain distribution in its three-dimensionality. The direction of the anisotropy planes in the sample is horizontal and

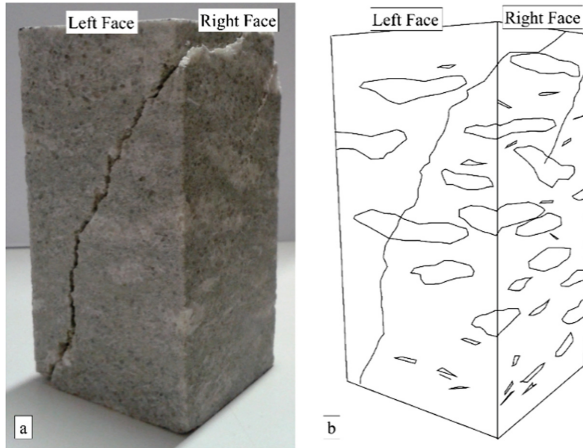


**Fig. 1.** a. Prismatic sample at the end of the Uniaxial Compression Test b. Schematic representation of the orientation of principal nodules and elongated gypsum crystals in the sample, underlining sub-horizontal planes of anisotropy and a preferential orientation parallel to the right face.

the elongation of gypsum crystals underlines a preferential orientation parallel to the right face (Fig. 1).

The uniaxial test was performed with a GDS Instruments Medium Pressure Triaxial Apparatus (MPTA): it was adapted to work without the triaxial cell, therefore functioning by applying only the compression to the sample and leaving it visible. Stress was applied with a constant strain rate of  $10^{-5}\text{s}^{-1}$ . Axial displacements of the entire sample (total displacements) were measured with LVDT sensors.

Videos (frame rate: 24 frames/s, with resolution of  $1920 \times 1080$  and focal length of 20 mm) were acquired throughout the test with two digital cameras (a Nikon D7000 and a Sony NEX-5N). Two adjacent and perpendicular faces were chosen in order to have a complete description of the deformation and failure of the sample.

One frame every 5 s was extracted from the videos and processed with Ncorr v.1.1.2.2 (Blaber et al. 2015), as described in Caselle et al. (2019). The result is the assignment of a strain value every 5 s for each point of the grid on the sample surface.

### 3 Results and Discussion

Stress-strain curve obtained from the uniaxial test is shown in Fig. 2a and 3a. The unconfined compressive strength of the sample is 22.09 MPa.

The curve shows the presence of a first phase that can be considered as elastic (point A). The elastic conditions are interrupted at the onset point (B), when strain rate increases until reaching the peak point (C). The successive curve section is a quite long post-peak phase with increase of the strain and slight decrease of strength (points D, E,

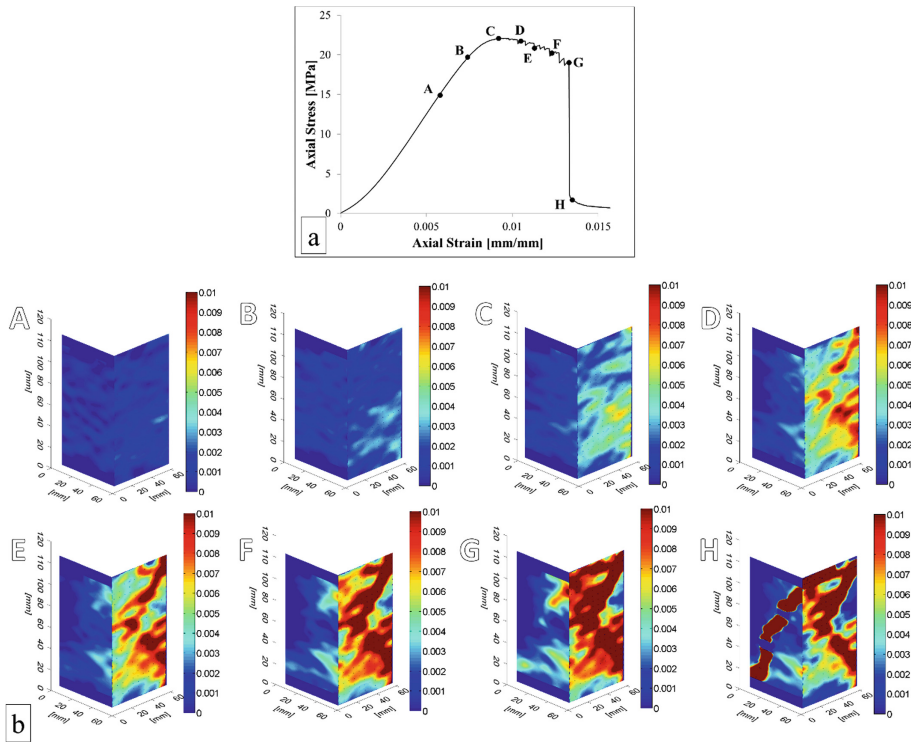


**Fig. 2.** a. Stress-strain curve. b. Axial strain maps of the two analyzed faces in correspondence to points from A to H.

F and G). This phase is characterized by several little stress drops. Eventually, between point G and point H, a sharp drop of strength leads to the real rupture of the sample.

From a macroscopic point of view, no evidences of failure can be recognized at point C (peak strength). The right face shows the first cracks at point F. Some further cracks, oriented as conjugated, are observable at point G and, more evidently, at the end of the test (point H). On the left face, no evidences of failure are recognizable until point H, after the stress drop, when the development of the principal failure surface is observable. However, the two parts of the sample remain in contact even after point H (see Fig. 1a) allowing for the acquisition of coherent photographic images up to the end of the test.

Figure 2b and Fig. 3b show the axial strain maps and horizontal strain maps, respectively, of the two analysed faces in points from A to H. Maps are reported on 3D graphs and oriented as in the real sample and the axial load direction corresponds to the z-axis. A uniform colour scale was chosen to facilitate the comparison. In this representation, compressive strains are considered as positive, while extensive strains are negative.

During the elastic phase, strains can be considered as homogeneous on the two faces. When the onset is reached (point B), we start to recognize the intensification of

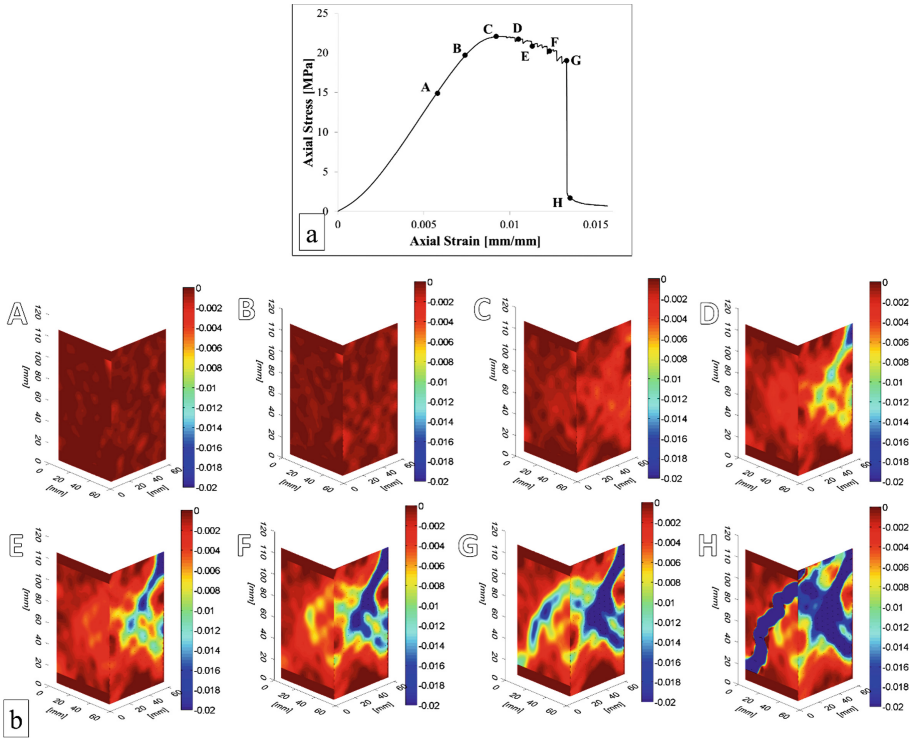


**Fig. 3.** a. Stress-strain curve. b. Horizontal strain maps of the two analyzed faces in correspondence to points from A to H.

axial strains in the lowest part of the right face. This element is enhanced when the peak is reached (point C). At this point, also the horizontal deformation shows a concentration of high strains, delineating the first evidences of two conjugated alignments. Similar evidences can be found on the left face only after the peak, at point D.

The following evolution of the sample continues to be characterized by a higher deformation on the right face than on the left face. However, the deformation on the right face does not bring to the complete failure of the sample, as shown by the stress-strain curve: little stress drops are quickly recovered, maintaining a constant stress/strain ratio. The significant increase of strain concentration on this face is insufficient to reach the failure of the sample.

On the other hand, when on the left face the alignment of horizontal strains covers the entire sample surface (Fig. 3b-point G), the sample fails, with an important stress drop (point H) and the clear formation of a well-defined failure surface. The direction of the final failure is therefore aligned with the linear anisotropy of the material.

The creation of a coherent failure surface able to suddenly reduce rock strength is allowed only in the direction parallel to the crystals elongation. The preferential orientation of gypsum crystals inhibits the coalescence of the strain concentrations located on the right face, where a real failure surface cannot be created.

Axial deformation maps (Fig. 2b) in correspondence of points F-G-H clearly show, in the lower right corner of the left face, the presence of a horizontal concentration of strains, better highlighted in Fig. 4a, that is concord with the anisotropy structure of the material. Looking at the picture of the sample (Fig. 4b) it is possible to recognize a structure (fine layer surrounding a nodule of gypsum crystals) oriented exactly as the strain concentration recognized in the strain map. The corresponding maps of horizontal strains (Fig. 3b-points F-G-H) highlight the presence, in the same position, of a conjugate structure, which seems to be, therefore, significantly controlled by the texture and structure of the material.

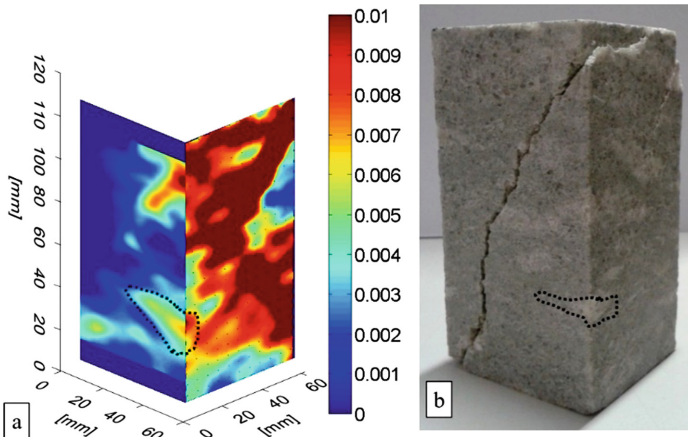


**Fig. 4a.** Axial strain map in correspondence of point G. **b.** Post-test sample. Note the presence of a horizontal concentration of strain (highlighted by the black line in Fig. 4(a)) and the correspondent nodule of clear gypsum crystals in the sample (black line in Fig. 4(b)).

A texture/structure control of the deformation and failure of the sample is evident also for the principal failure surfaces. The deformation starts with a high axial strain, not uniform, but horizontally stratified, following the anisotropy of the material. Afterwards, horizontal strains concentrations can be visualized. The strains seem to maintain this horizontal inhomogeneity for all the test. The subsequent coalescence of the concentrations of horizontal strains brings, eventually, to the formation of the failure surface.

## 4 Conclusions

Mechanical properties of rock materials influence the mining and engineering design. The UCS value is sometime insufficient to describe the evolution of the rock behaviour. Rock structures in underground mine or tunnelling, as for example walls and pillars, are subjected to a deformative evolution under load and local effects are observable on the surface of the rock.

The present study aims to underline the potentialities and the advantages of the application of DIC analysis methodology on two adjacent faces of rock samples. Without interfering with the evolution of a standard Uniaxial Compression Test, DIC analysis provides a large quantity of additional information: measurement of local strains in axial and horizontal directions on the entire surface of the sample can be obtained without the use of additional sophisticated and expensive laboratory tools. The investigation of two faces of prismatic samples allows for a three-dimensional description of strain evolution, particularly important if the material is inhomogeneous and anisotropic.

Textural and structural features of the gypsum here tested are similar at the mesoscale and at the sample scale, so the experiments can simulate the behaviour of a loaded pillar, showing its strain evolution.

Maps of strain concentrations at different stress levels can be created and used for a more thought interpretation of material behaviour. Anomalous strain concentrations may be interpreted considering the structure and texture features of the original material. As a result, the analysis of rock behaviour will keep in consideration the peculiarities of the specific rock, with its own anisotropies, inhomogeneities and textural variations. Potential weakness layers can be recognized in association with the textural variations. The influence of these peculiarities of the rock on the mechanical behaviour at the laboratory scale, but also at the rock-mass scale, is often a key factor in the stability assessment.

The combination of these features and the additional information provided by DIC analysis suggest the utility of this methodology in the characterization of mechanical properties of intact rock. The method provides more complete and useful results than the simple stress-strain curve of the UCS test without increasing cost, number or features of performed tests.

## References

- Blaber J, Adair B, Antoniou A (2015) Ncorr: open-source 2D digital image correlation matlab software. *Exp Mech* 55:1105–1122. <https://doi.org/10.1007/s11340-015-0009-1>
- Caselle C, Umili G, Bonetto S, Ferrero AM (2019) Application of DIC analysis method to the study of failure initiation in gypsum rocks. *Géotech Lett* 9:1–21. <https://doi.org/10.1680/jgele.18.00156>
- Chu TC, Ranson WF, Sutton MA (1985) Applications of digital-image-correlation techniques to experimental mechanics. *Exp Mech* 25:232–244. <https://doi.org/10.1007/BF02325092>
- Ferrero AM, Migliazza MR (2009) Theoretical and numerical study on uniaxial compressive behaviour of marl. *Mech Mater* 41:561–572. <https://doi.org/10.1016/j.mechmat.2009.01.011>
- Lugli S, Vinicio M, Marco R, Charlotte SB (2010) The Primary Lower Gypsum in the Mediterranean: A new facies interpretation for the first stage of the Messinian salinity crisis. *Palaeogeogr Palaeoclimatol Palaeoecol* 297:83–99. <https://doi.org/10.1016/j.palaeo.2010.07.017>
- Nguyen TL, Hall SA, Vacher P, Viggiani G (2011) Fracture mechanisms in soft rock: Identification and quantification of evolving displacement discontinuities by extended digital image correlation. *Tectonophysics* 503:117–128. <https://doi.org/10.1016/j.tecto.2010.09.024>



- Peters WH, Ranson WF (1982) Digital imaging techniques in experimental stress analysis. *Opt Eng* 21:427–431. <https://doi.org/10.1117/12.7972925>
- Stirling RA, Simpson DJ, Davie CT (2013) The application of digital image correlation to Brazilian testing of sandstone. *Int J Rock Mech Min Sci* 60:1–11. <https://doi.org/10.1016/j.ijrmms.2012.12.026>
- Vend Roux G, Knauss WG (1998) Submicron deformation field measurements: Part 2. Improved digital image correlation *Exp Mech*. 38:86–92. <https://doi.org/10.1007/BF02321649>
- Vitone C, Viggiani G, Cotecchia F, Hall SA (2013) Localized deformation in intensely fissured clays studied by 2D digital image correlation. *Acta Geotech* 8:247–263. <https://doi.org/10.1007/s11440-013-0208-9>
- Yang G, Cai Z, Zhang X, Fu D (2015) An experimental investigation on the damage of granite under uniaxial tension by using a digital image correlation method. *Opt Lasers Eng* 73:46–52. <https://doi.org/10.1016/j.optlaseng.2015.04.004>
- Zhang H, Huang G, Song H, Kang Y (2012) Experimental investigation of deformation and failure mechanisms in rock under indentation by digital image correlation. *Eng Fract Mech* 96:667–675. <https://doi.org/10.1016/j.engfracmech.2012.09.012>